Applied Energy 88 (2011) 5173–5179

Contents lists available at SciVerse ScienceDirect

Applied Energy

journal homepage: www.elsevier.com/locate/apenergy

An effective Seebeck coefficient obtained by experimental results of a thermoelectric generator module

Cheng-Ting Hsu [a,b], Gia-Yeh Huang [c], Hsu-Shen Chu [b], Ben Yu [d], Da-Jeng Yao [a,c,*]

[a] Institute of NanoEngineering and MicroSystems, National Tsing Hua University, Hsinchu 30013, Taiwan, ROC
[b] Material and Chemical Research Laboratories, Industrial Technology Research Institute, Hsinchu, Taiwan, ROC
[c] Department of Power Mechanical Engineering, National Tsing Hua University, Hsinchu 30013, Taiwan, ROC
[d] Wise Life Technology Co. Ltd., Hsinchu, Taiwan, ROC

ARTICLE INFO

Article history:
Received 8 March 2011
Received in revised form 18 July 2011
Accepted 18 July 2011
Available online 20 August 2011

Keywords:
Seebeck coefficient
Temperature dependence
Thermoelectric generator
TEG module
Contact effect
Thermal resistor network

ABSTRACT

This article proposes a concept of "effective Seebeck coefficient", which discusses the inconsistency between the theoretical Seebeck coefficient and the measured one. The inconsistency can be explained via contact effect and thermal resistor network. Two different clamping forces are applied to the TEG module to observe the contact effect. Throughout the experiments, the electric resistance seems insensitive to the clamping force; somehow the thermal contact effect dominates the TEG module performance. In addition, a thermal resistor network, which is used to calculate the exact temperature difference traverse the TE ingot, has been constructed. After applying a suitable clamping pressure and modifying the actual ΔT with thermal resistor network, the "effective Seebeck coefficient" has been proposed. Notably, this proposed value is very helpful for better understanding characteristics of the behavior of the TEG module operating in the actual conditions we provided, and it can be used to predict the performance of the TEG module under any other condition.

1. Introduction

Bismuth telluride (Bi-Te) is the most easily obtained commercially available thermoelectric materials for the present. The range of operating temperature is from room temperature to 250 °C. It is very suitable for the application of low-temperature waste heat recovery [1–10]. In most cases, manufacturers of thermoelectric generator (TEG) modules provide datasheets which are including the performance curves such as maximum output voltage (V_{max}), maximum output current (I_{max}), maximum absorbed heat energy (Q_{max}), and maximum output power (P_{max}), at several testing conditions. However, details about the interior parameters of the TEG module, such as dimensions of P–N ingot, Seebeck coefficient (α), electric resistance (R), thermal conductivity (K) and figure of merit (ZT), are not available. Therefore, two methods to obtain the interior parameters are suggested. One is to conduct the measured material parameters experimentally by destruction of TEG module. The other is to conduct the best performance value according to the measurements provided by manufacturer to calculate the interior parameters. Although damaging the TEG module to measure the interior parameters of one TE couple is a direct measurement method which represents the actual behavior of this TE material, it is not recommended due to the costly TEG module. Thence, Luo proposed two mathematical approaches to obtain the interior parameters of a thermoelectric cooler (TEC) module based on vendor's datasheets: method I uses maximum output voltage (V_{max}), maximum output current (I_{max}) and maximum temperature difference (ΔT_{max}) while method II uses maximum absorbed heat energy (Q_{max}), maximum output current (I_{max}) and maximum temperature difference (ΔT_{max}) to obtain the interior thermoelectric material parameters. However, these two methods did not completely match the basic thermoelectric equations. That is, the two methods show about 5% inconsistency when comparing to each other [11]. Because TEC and TEG module share the same thermoelectric material parameters, Luo's researching results provide a good analysis method and can be applied in TEG parameters analysis as well.

How could an engineer simulate the performance of a TEG module without its interior parameter. Typically, the theoretical thermoelectric coefficients were applied in each specific simulation model. However, it could not reflect the practical working condition. Hence, Woo and Lee proposed a methodical technique, which constructed a simulation model based on experimental results to predict the TEG performance more precisely. But the temperature dependence of TE material properties had not been considered [12].

Hsiao et al. have constructed a mathematic simulation model, based on the testing results of a TEG module, to predict the

* Corresponding author at: Institute of NanoEngineering and MicroSystems, National Tsing Hua University, Hsinchu 30013, Taiwan, ROC. Tel.: +886 3 5715131x42850.
E-mail address: djyao@mx.nthu.edu.tw (D.-J. Yao).

0306-2619/$ - see front matter © 2011 Elsevier Ltd. All rights reserved.
doi:10.1016/j.apenergy.2011.07.033

performance of a waste heat recovery system. They provided a scientific methodology with complicated formulas on the field of thermoelectric simulations [13], which was very impressive.

Another factor that influences the performance of TEG module but did not model in classical thermoelectric theory is thermal contact effect. While measuring the performance of a TEG module, it is helpful to apply a clamping force to reduce thermal resistance between each interface. Predicated on this study and our previous research [14,15], it is suggested to apply an appropriate pressure on a TEG module to improve the performance.

Practically, the working conditions of TEG module are not always in an extreme operation conditions. Namely, if one would like to predict the performance of a TEG module, or even to predict the system performance that connects several TEG modules, it will likely be overvalued if the extreme value, such as Q_{max}, V_{max}, I_{max} and ΔT_{max} were applied. Apart from the above two approaches, a direct experimental method is presented in this work. Commercially available Bi_2Te_3 TEG modules are examined by several points of experiments and verified with theoretical results. The concept of "Effective Seebeck Coefficient" is proposed which offers an important indicator of TEG system performance. Theoretical analysis and experimental procedures will be explained in the following sections.

2. Basic theory of TEG

The working principles of TEG are based on its thermoelectric effect, which are Seebeck effect, conduction effect and Joule effect. Take a single TE couple for example, as a heat source applies heat energy Q_h (W) to create a temperature difference ΔT (K) between both sides of the P–N ingot. The electrical current I (A) is induced in the circuit. For the conduction effect in this case, the amount of power is proportional to the thermal conductivity K ($W K^{-1}$) and temperature difference $\Delta T = T_h - T_c$ (K). As the electrical current going through the TE leg, Joule heat is generated internally, which is proportional to the electrical resistance R (Ω) and the square of the current. Joule heat is considered to heat both hot and cold side in the same amount. Fig. 1 illustrates the formation of induced electrical current inside the TEG model which is composed of P- and N- TE couple, electrical conductor (Cu), and ceramic plates. Besides, internal material properties are supposedly constant that independent of temperature and no heat losses are assumed. The rate of supply heat Q_h and removal heat Q_c can be estimated at the hot and cold junction respectively.

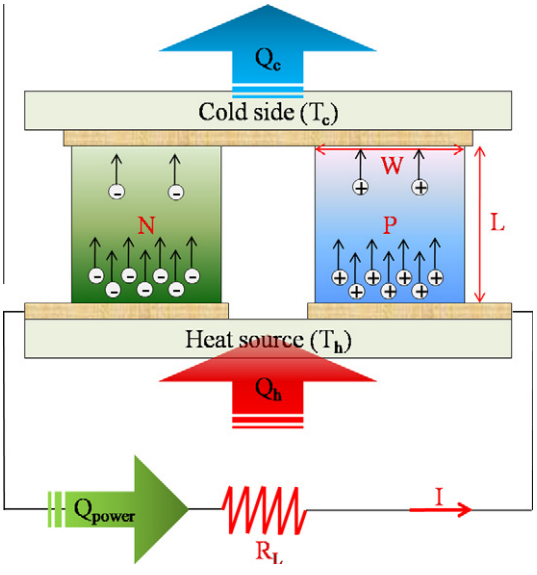

Fig. 1. Illustrates the formation of induced electrical current inside the TEG model.

$$Q_h = (K_p + K_n)(T_h - T_c) + (\alpha_p - \alpha_n)IT_h - \frac{I^2R}{2} \quad (1)$$

$$Q_c = (K_p + K_n)(T_h - T_c) + (\alpha_p - \alpha_n)IT_c + \frac{I^2R}{2} \quad (2)$$

in which K_p and K_n are thermal conductivity of P- and N-type TE leg, T_h and T_c represent the hot and cold junction temperature, and α_p and α_n are the Seebeck coefficient of P- and N-type TE leg respectively.

Referring to Fig. 1, the electrical power generated by TEG is simply the form of the voltage across the external load and current in the circuit. According to the power balance equations, electrical power can be obtained.

$$W = Q_h - Q_c = V \cdot I \quad (3)$$

Rearranging Eqs. (1)–(3)

$$(\alpha_p - \alpha_n)I(T_h - T_c) - I^2R = V \cdot I \quad (4)$$

Both sides of Eq. (4) divided by I

$$V = (\alpha_p - \alpha_n)(T_h - T_c) - IR \quad (5)$$

Simplifying Eq. (5), and let $\alpha = (\alpha_p - \alpha_n)$ and $\Delta T = (T_h - T_c)$:

$$V = \alpha\Delta T - IR \equiv A\Delta T - BI \quad (6)$$

Eq. (6) implies that the output voltage as a function of the current for a given temperature differences. Furthermore, for the open circuit voltage, that is, $I = 0$ in Eq. (6), $A\Delta T$ has a maximum value in which A is defined as the "effective Seebeck coefficient":

$$A = \frac{V}{\Delta T} \quad (7)$$

where V is the open circuit voltage when $I = 0$. Therefore, the value of A becomes a very important indicator which is expressing the behavior of the TEG module operating in the actual conditions we provided. Otherwise, the value of B will be the slope that represents the matching load of a TEG module. In short, Eq. (6) becomes the significant indicator to characterize the performance of a TEG module or a system that composed of TEG modules.

3. Measurement

To demonstrate the concept of this specific study, geometric features and transport properties of a TE couple should be tabulated as a reference, which helps to compare with experimentally measured data. Therefore, the associated geometric features and material properties at 300 K—which were provided by vender datasheets—are listed in Table 1.

3.1. TEG module testing

A TEG module (TMH400302055, Wise Life Technology, Taiwan) with 199 TE couples has been employed in this experiment. A measuring system, which equipped a sandwiched structure (from top to bottom) of heater/copper plate/TEG module/copper plate/liquid cooling system, was conducted for a single TEG module testing, as shown in Fig. 2. When staring this specific experiment, the TEG module was clamped between two copper plates. The copper plates were treated as heat spreaders to provide a uniform thermal field to both hot and cold sides of TEG module. Besides, two thermocouples were inserted into these two copper plates respectively to measure the temperature difference between the hot and cold sides of a TEG module. Moreover, a pressure gage was applied to

Table 1
Geometric features and transport properties of a TE couple.

Parameter at 300 K	N-type element	P-type element	Copper	Ceramic	Solder	Thermal grease
Seebeck coefficient ($V\,K^{-1}$)	-2.12×10^{-4}	2.15×10^{-4}	N/A	N/A	N/A	N/A
Resistivity (Ω m)	1.04×10^{-5}	1.04×10^{-5}	3.2×10^{-8}	1×10^{12}	12.1×10^{-8}	N/A
Thermal conductivity ($W\,m^{-1}\,K^{-1}$)	1.456	1.373	385	22	50	3
Z (K^{-1})	2.97×10^{-3}	3.23×10^{-3}	N/A	N/A	N/A	N/A
Thermal resistivity ($K\,W^{-1}$)	109.89	116.79	0.1443	3.207	0.25	0.74
Contact area (m^2)	4×10^{-6}	4×10^{-6}	9×10^{-6}	9×10^{-6}	4×10^{-6}	9×10^{-6}
Thickness (m)	6.4×10^{-4}	6.4×10^{-4}	5×10^{-4}	6.35×10^{-4}	5×10^{-5}	2×10^{-5}

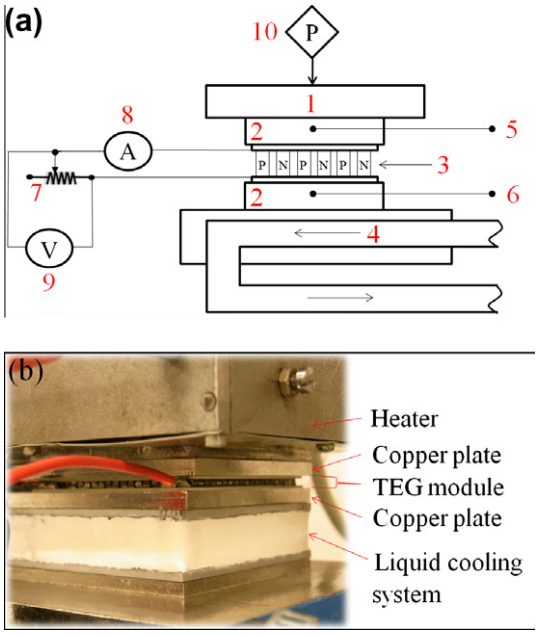

Fig. 2. Schematic diagram of the experimental system: (a) 1: Heater. 2: Copper plate. 3: TEG module. 4: Liquid cooling system. 5: Thermal couple for hot side. 6: Thermal couple for cold side. 7: Tunable high power electrical resistor array. 8: Ammeter. 9: Voltmeter. 10: Pressure gauge. (b): The entity chart of the experimental system.

control the clamping force to the TEG module; the coolant (water) was supplied from a water-circulating chiller to maintain a cold-side temperature (T_c), the architecture of this experiment is shown in Fig. 2a. As a selected temperature difference (ΔT) applied to a TEG module after turning on the heater and water-circulating system, the open-circuit voltage (V_{oc}) has been recorded until a stable ΔT. Thereafter, the external load voltage (V_L) could be obtained by the data acquisition system when applying an external load. Accordingly, the impedance matching point occurs when 1/2 V_{oc} was measured across the external load. Figs. 3 and 4 illustrate the measuring results of each individual V_L versus power output (P) for different ΔT, where V_L is tunable by means of the data acquisition system, and ΔT refers temperature difference between both sides of the TEG module. Besides, different hot side temperature (T_h) of TEG module has been set from 310 to 370 K with 10 K increment to further study the temperature dependence of material properties.

Referring to the results of Figs. 3 and 4, maximum power outputs of each case are obtained expectably when V_L adjusted to 1/2 V_{oc}. Moreover, Figs. 5 and 6 describe the detailed information of voltage and current of each measured point in Figs. 3 and 4 respectively, which indicate in straight lines for different ΔT. Predicated on Eq. (6), these straight lines in Figs. 5 and 6 have specific physical meanings, that each slope represents the internal electrical resistance of the TEG module at the specific measuring

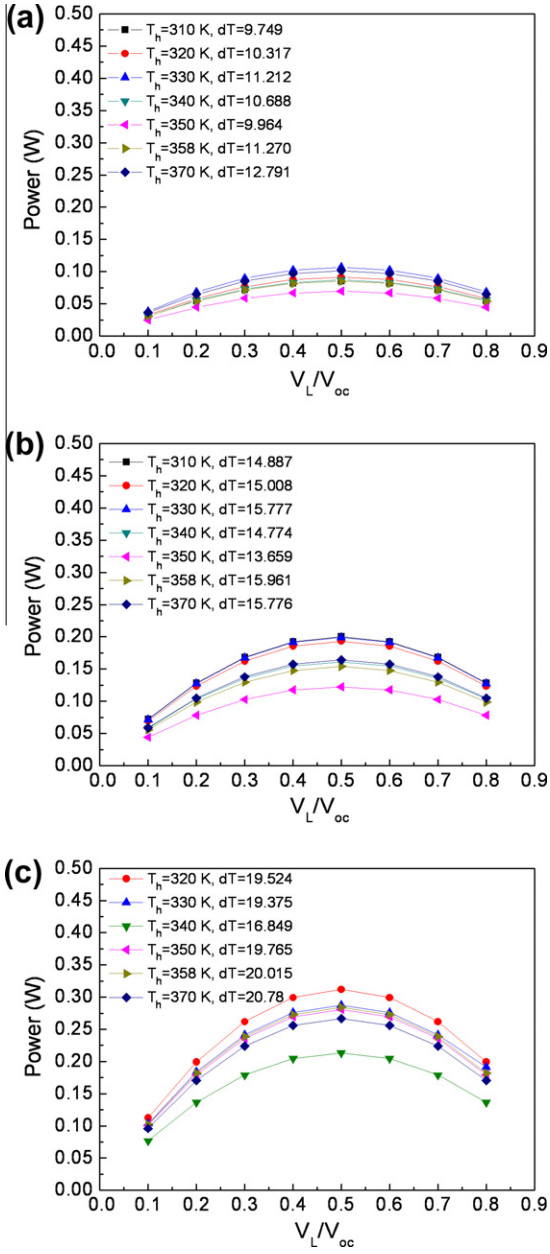

Fig. 3. Power output versus load voltage measuring results of a TEG module with clamping force 12 kg W (0.423 kg/cm^2) for different hot side temperature (T_h). (a): $\Delta T \sim 10$ K, (b): $\Delta T \sim 15$ K and (c): $\Delta T \sim 20$ K.

environment, and each interception represents the open circuit voltage of the TEG module while $I = 0$. It is worth mentioning that one must trace the ΔT more carefully and rigorously to deduce the significant parameter—effective Seebeck coefficient—more precisely. While processing these series of experiments, two different

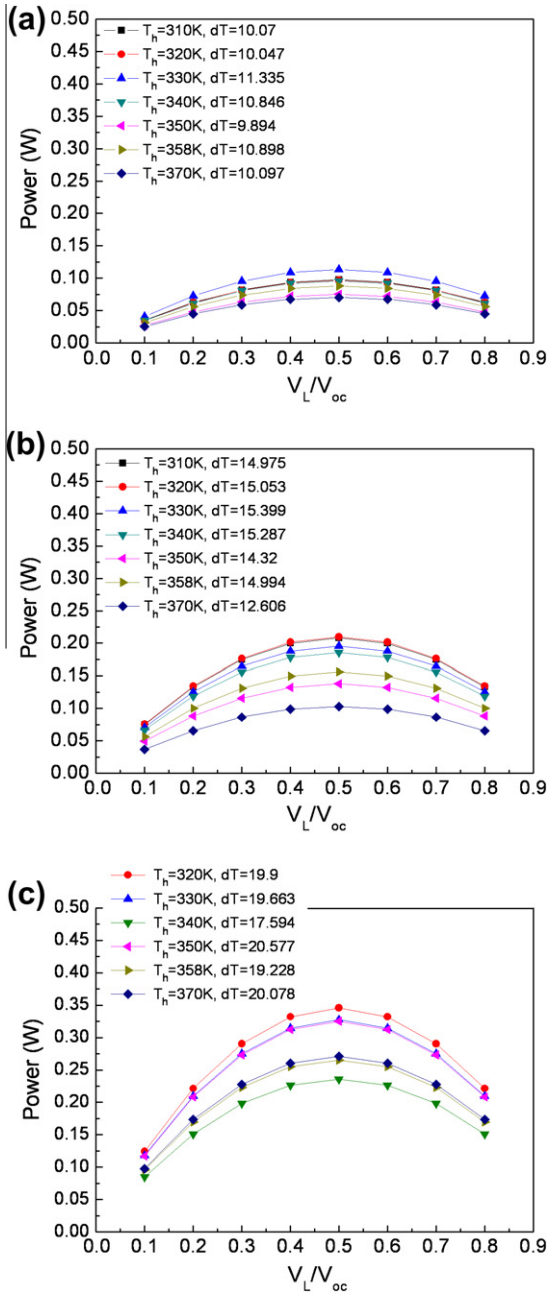

Fig. 4. Power output versus load voltage measuring results of a TEG module with clamping force 18 kg W (0.634 kg/cm^2) for different hot side temperature (T_h). (a): $\Delta T \sim 10$ K, (b): $\Delta T \sim 15$ K and (c): $\Delta T \sim 20$ K.

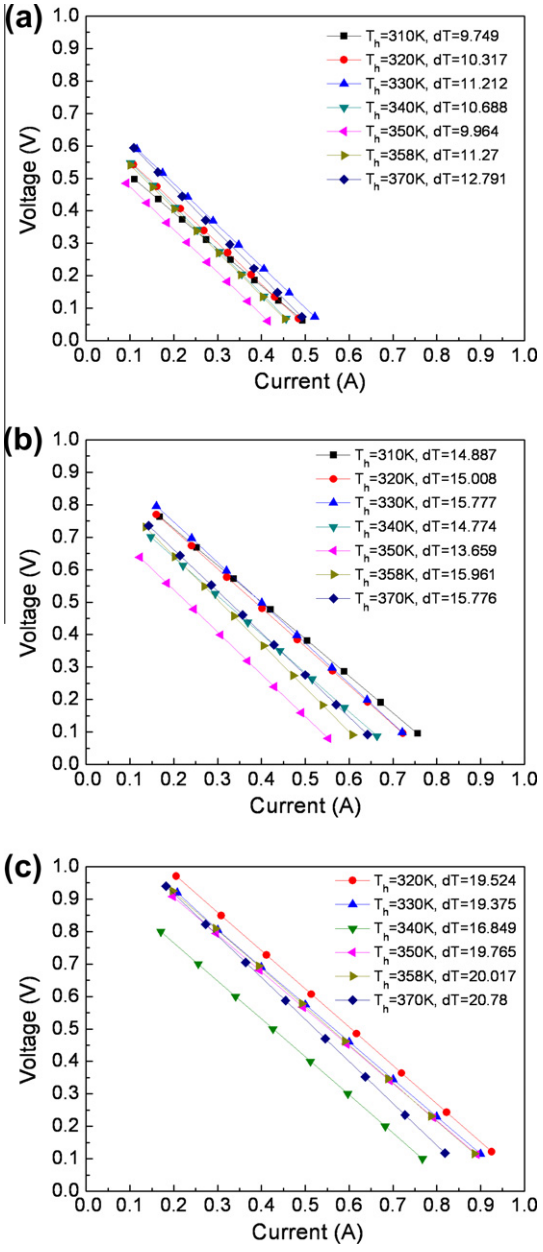

Fig. 5. Voltages versus current measurements from Fig. 3 with clamping force 12 kg W (0.423 kg/cm^2) for different hot side temperature (T_h). (a): $\Delta T \sim 10$ K, (b): $\Delta T \sim 15$ K and (c): $\Delta T \sim 20$ K.

pressure loads of 12 and 18 kg W (0.423 and 0.634 kg/cm^2 respectively) was applied to clamp the TEG module to discuss the issue of thermal contact effect.

In accordance with the measurements of different ΔT at particular hot side temperature in Figs. 5 and 6, the slope of each line, which represents the internal electrical resistance, can be obtained statistically by linear approximation, as shown in Tables 2 and 3. Through experiments with clamping force 12 and 18 kg W, the matching load is obtained from 1.134 to 1.359 Ω and 1.111–1.375 Ω respectively with increasing T_h from 310 to 370 K, this phenomenon is due to the temperature dependence of the material properties (electrical resistance) of TE element. The slope of each statistic data exhibits good agreement with the experimental results. Furthermore, for the open circuit voltage, that is, $I = 0$ in Eq. (6). The "effective Seebeck coefficient" can be consequently obtained according to Eq. (7), where V is the open circuit voltage that represents the interception of Y axial in Figs. 5 and 6. This specific parameter, effective Seebeck coefficient, expresses the behavior of the TEG module operating in the actual conditions we provided.

3.2. Results and discussion

Apparently, an interesting result comes out. Table 1 provides the Seebeck coefficient of a single TE couple which is considered as the theoretical value. Notably, the Seebeck coefficient falls off from the results of Table 1 through Table 3. Namely, if customers just applied the parameters in Table 1 instead of Table 2 and/or Table 3 to predict the performance of their specific TEG system, then they will overestimate it. For example, the Seebeck coefficient, $\alpha = (\alpha_p - \alpha_n)$, of one TE couple is 4.27×10^{-4} V K^{-1} (see Table

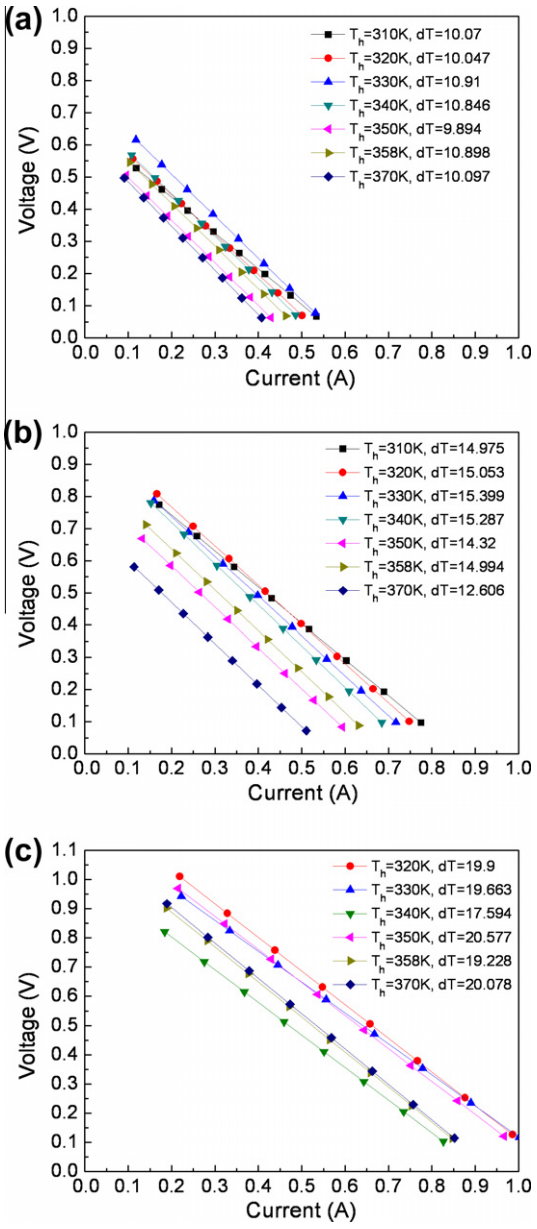

Fig. 6. Voltages versus current measurements from Fig. 4 with clamping force 18 kg W (0.634 kg/cm^2) for different hot side temperature (T_h). (a): $\Delta T \sim 10$ K, (b): $\Delta T \sim 15$ K and (c): $\Delta T \sim 20$ K.

Table 2
Statistics of the data in Fig. 5.

T_h (K)	Mean slope	S.D.	Mean α	S.D.
310	1.134	5.773E-4	0.06394	1.989E-4
320	1.212	0.04197	0.06398	0.0018
330	1.222	0.06437	0.06275	0.00325
340	1.237	0.09732	0.06088	0.0027
350	1.254	0.09387	0.05887	0.00177
358	1.291	0.1007	0.05833	0.00145
370	1.313	0.03955	0.05751	0.00115

S.D. signifies "Standard Deviation", α signifies "Effective Seebeck Coefficient".

1) at 300 K. There are 199 TE couples integrated in a module. Theoretically, the calculated the Seebeck coefficient of one TEG module should be $4.27 \times 10^{-4} \times 199 = 0.0849$ V K^{-1}. Comparing the theoretical value with the measured one, there is more than 30% of

Table 3
Statistics of the data in Fig. 6.

T_h (K)	Mean slope	S.D.	Mean α	S.D.
310	1.116	0.00707	0.06497	6.607E-4
320	1.206	0.04957	0.06661	0.00293
330	1.200	0.12689	0.06391	0.00401
340	1.238	0.10659	0.06253	0.00376
350	1.241	0.10166	0.06039	0.00303
358	1.264	0.06265	0.06020	0.00209
370	1.289	0.08229	0.05876	0.00248

S.D. signifies "Standard Deviation", α signifies "Effective Seebeck Coefficient".

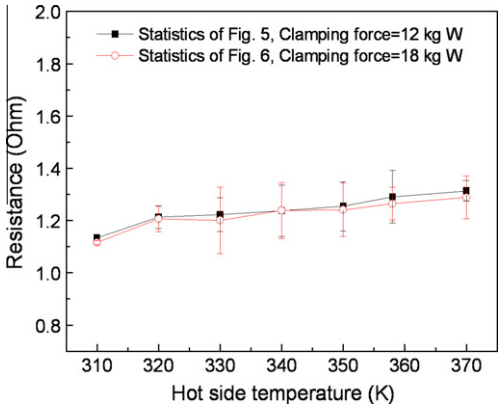

Fig. 7. Juxtaposed data of slope (resistance) statistics under two different clamping forces based on Figs. 5 and 6 (or Tables 2 and 3).

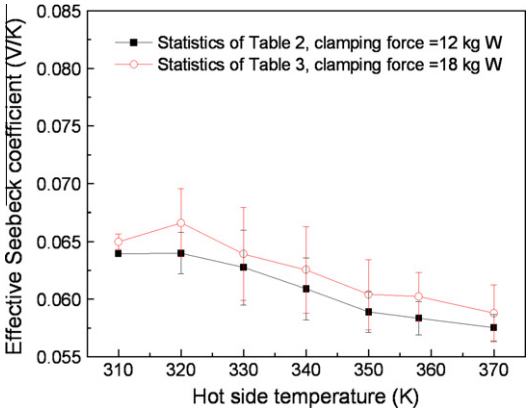

Fig. 8. Juxtaposed data of effective Seebeck coefficient statistics under two different clamping forces based on Tables 2 and 3.

inconsistency has been notified. The measured "Mean α" in Tables 2 and 3 can be characterized as "effective Seebeck coefficient" which is expressing the behavior of the TEG module operating in the actual conditions we provided.

To further study of the inconsistency, two major possible reasons are concluded to explain the decline phenomenon, which are (1) contact effect and (2) thermal resistor network analysis.

3.2.1. Contact effect

To discuss the contact effect, two different clamping forces were applied to the TEG module while the same measuring system has been investigated in the previous section. Predicated on the past experience, the maximum clamping force should not exceed 18 kg W (0.634 kg/cm^2); otherwise TEG module will be damaged.

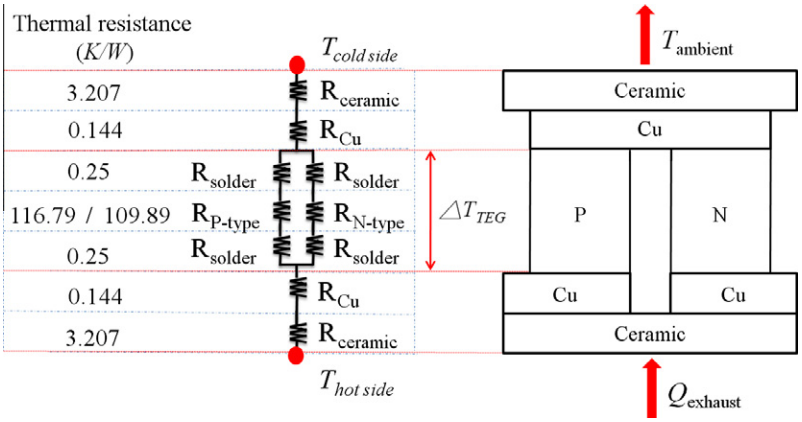

Fig. 9. Thermal resistor network with a single TE couple.

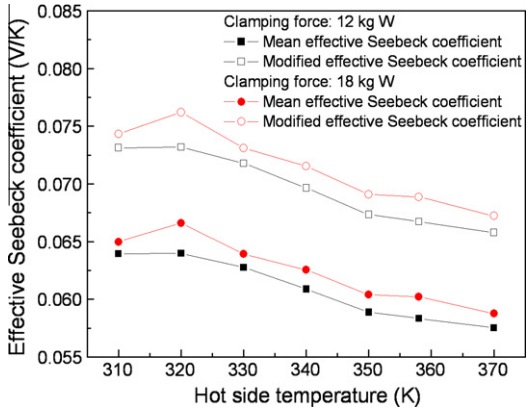

Fig. 10. The measured and modified effective Seebeck coefficient with a TEG module under two different clamping force.

Therefore, a loosed clamping force of 12 kg W (0.423 kg/cm^2) was equipped. Fig. 7 shows the juxtaposed data of slope statistics under two different clamping forces based on Figs. 5 and 6 (or Tables 2 and 3). Consistent with Eq. (6), the slope signifies the internal resistance of a TEG module at a particular T_h. The solid dots indicate the measured results under clamping force of 12 kg W (0.423 kg/cm^2) while the hollow ones represent the clamping force of 18 kg W (0.634 kg/cm^2).

Fig. 8 shows another juxtaposed data of effective Seebeck coefficient statistics under two different clamping forces based on Tables 2 and 3. Consistent with Eq. (7), the effective Seebeck coefficient of a TEG module is thus deduced at a particular T_h. The solid dots indicate the measured results under clamping force of 12 kg W (0.423 kg/cm^2) while the hollow ones represent the clamping force of 18 kg W (0.634 kg/cm^2). From the experimental results in this specific case, the maximum value of the apparent Seebeck coefficient is at 320 K, and the apparent Seebeck coefficient drop observably at high temperature region. This anticipated result exhibits good agreement with the fundamental material properties of Bi_2Te_3.

Generally speaking, a greater temperature difference increases the generated power; however, the performance of a thermoelectric element decreases at high temperature region because of the temperature dependence of the material properties. Throughout the experiments, both of the electrical resistance and effective Seebeck coefficient varying with different T_h has been observed. The electrical resistance is seemingly the same whether 12 or 18 kg W clamping force was applied. Conversely, the effective Seebeck coefficient is slightly superior as clamping force of 18 kg W to that of 12 kg W. To decrease the thermal contact effect, applying an appropriate pressure on a TEG module is suggested to improve the performance.

3.2.2. Thermal resistor effect

To observe a precisely effective Seebeck coefficient, temperature difference (ΔT) was recorded carefully and rigorously through Figs. 3–6. Albeit the thorough measured ΔT, it is not the exact temperature difference traverse the TE ingot. Hence a thermal resistor network has been constructed. According to the analysis of the thermal resistor network in Fig. 9, the exact ΔT cross TE ingot, ΔT_{TEG}, is calculated with Eq. (8) in accordance with measured values T_h and T_c, which enables us to predict the performance more precisely [14,15].

$$\Delta T_{TEG} = \frac{(R_N + 2R_{sol})//(R_P + 2R_{sol})}{2(R_{cer} + R_{Cu}) + (R_N + 2R_{sol})//(R_P + 2R_{sol})} \times (T_h - T_c) \quad (8)$$

in which T_h and T_c are measured temperatures at the hot and cold side of the TEG module respectively. Moreover, all parameters such as dimensions and material properties are tabulated in Table 1, and the thermal resistance of each component is described on the left of Fig. 9. Perfect contact at each interface has been assumed in this case. According to Eq. (8), the relation between ΔT_{TEG} and $(T_h - T_c)$ should be concluded as

$$\Delta T_{TEG} = 0.8742(T_h - T_c) \quad (9)$$

and the modified effective Seebeck coefficient (α') is

$$\alpha' = \frac{V}{\Delta T_{TEG}} = \frac{V}{0.8742(T_h - T_c)} \quad (10)$$

Now, reconsidering ΔT_{TEG} in accordance with Eq. (9), a modified effective Seebeck coefficient predicated in Eq. (10) is investigated, as shown in Fig. 10, while the mean effective Seebeck coefficient is the statistic results described in Tables 2 and 3. This significant modification provides an analytical method to discover the value of α', which is more approaching to the theoretical value.

At first glance, there is more than 30% inconsistency between theoretical Seebeck coefficient and the measured one. After applying a suitable clamping pressure and modifying the actual temperature difference (ΔT_{TEG}) with thermal resistor network, the modified effective Seebeck coefficient has been proposed. This proposed value is a very important indicator which is expressing the behavior of the TEG module operating in the actual conditions we provided, and it can be used to predict the performance of the TEG module under any other condition.

4. Conclusion

The common problem of the TEG module level applications is that the theoretical material properties are typically superior to the practical ones. The objective of this study is to identify this problem, to correct it experimentally and finally to propose a concept of "effective Seebeck coefficient". Compared the theoretical Seebeck coefficient with the measured one, the inconsistency can be understood by considering the contact effect and thermal resistor network, which are not modeled in classical theory. To address these issues, this study investigates the thermal contact effect which is shown to dominate the thermal electrical properties including the "effective Seebeck coefficient". Besides, temperature dependence of material properties has been examined. Although the TEG module is under a fixed hot side temperature, the electrical resistance and the effective Seebeck coefficient show a discrepancy with different cold side temperature. To minimize the error in this analytical method, measuring at the same point for several times to achieve an averaged data is necessary.

Acknowledgment

National Science Council (NSC Project No. NSC-98-3114-E-007-008) supported this project and gave technological assistance.

References

[1] Niu X, Yu J, Wang S. Experimental study on low-temperature waste heat thermoelectric generator. J Power Sources 2009;188:621–6.
[2] Hsu CT, Huang GY, Chu HS, Yu B, Yao DJ. Experiments and simulations on low-temperature waste heat harvesting system by thermoelectric power generators. Appl Energy 2011;88:1291–7.
[3] Gou X, Xiao H, Yang S. Modeling, experimental study and optimization on low-temperature waste heat thermoelectric generator system. Appl Energy 2010;87:3131–6.
[4] Champier D, Bedecarrats JP, Rivaletto M, Strub F. Thermoelectric power generator from biomass cook stoves. Energy 2010;35:935–42.
[5] Talom HL, Beyene A. Heat recovery from automotive engine. Appl Therm Eng 2009;29:439–44.
[6] Rowe DM. Thermoelectrics hankbook – macro to nano. Boca Raton, FL: CRC-Taylor & Francis; 2006.
[7] Rowe DM. Thermoelectrics, an environmentally-friendly source of electrical power. Renew Energy 1999;16:1251–6.
[8] Rowe DM, Min G. Evaluation of thermoelectric modules for power generation. J Power Source 1998;73:193–8.
[9] Rowe DM. Development of improved modules for the economic recovery of low temperature waste heat. In: Proc Int Conf Thermoelectrics Dresden, Germany; 1997.
[10] Rowe DM, Min G. Optimisation of thermoelectric module geometry for waste heat electrical power generation. J Power Source 1991;38:253–9.
[11] Luo Z. A simple method to estimate the physical characteristics of a thermoelectric cooler from vendor datasheets. Electron Cooling 2008;14:22–7.
[12] Woo BC, Lee HW. Relation between electric power and temperature difference for thermoelectric generator. Int J Modern Phys B 2003;17:1421.
[13] Hsiao YY, Chang WC, Chen SL. A mathematic model of thermoelectric module with applications on waste heat recovery from automobile engine. Energy 2010;35:1447–54.
[14] Yao Da-Jeng, Yeh Ke-Jyun, Hsu Cheng-Ting, Yu Ben-Mou, Lee J-S. Efficient reuse of waste energy. IEEE Nanotechnol Magazine 2009;3:28–33.
[15] Hsu CT, Yao DJ, Ye KJ, Yu BM. Renewable energy of waste heat recovery system for automobiles. J Renew Sustain Energy 2010;2.